NEW ELEMENTAL ABUNDANCE MAPS INTEGRATING OPTICAL AND GEOCHEMICAL DATA ON THE LUNAR SURFACE

Vadym Kaydash, Yuriy Shkuratov, Vitaliy Omelchenko, Dmitry Stankevich

Astronomical Institute of Kharkov National University, 35 Sumskaya St., Kharkov 61022, Ukraine
E-mail: kvg@vk.kh.ua

ABSTRACT

We present new maps of chemical elements abundances over the lunar surface. We propose a technique that interpolates available chemical elements distributions obtained by Lunar Prospector (1999) Gamma-ray spectrometer using Clementine (1994) UVVIS spectral reflectance images. Our main idea is to use low resolution GRS data as a "Ground truth" to establish relationships linking optical mineralogy and geochemical information. Then the relationships and Clementine UVVIS data are used to derive elemental abundance maps with significantly improved spatial resolution, up to 10 times. As an illustration of the suggested technique, maps for the elements Fe, Ti, Al, Ca, Mg, and O with pixel size 15 km x 15 km are presented. New maps for the chemical elements appear to be informative. For instance, the map of oxygen abundance demonstrates an anomaly in the crater Tycho, and the map of calcium shows fairly low mare/highland contrast.

INTRODUCTION

The chemical elements Si, O, Fe, Ti, Al, Ca, and Mg are major elements in the lunar rocks and soils. Information about the abundance and distribution of these and some other elements over the lunar surface was obtained with different remote sensing techniques: gamma-ray, X-ray, and optical spectroscopy. Global gamma-ray (GRS) and neutron spectrometers data were acquired during the low- and high-altitude portions of the Lunar Prospector mission [1,2]. The data were presented as preliminary maps with different sizes of pixels, respectively, 0.5° x 0.5° (15 km x 15 km at the equator) and 5° x 5° (150 km x 150 km at the equator). The initial GRS data went through complicated processing. At the present time, the current maps are unique determinations of the lunar surface composition, i.e. distributions of Si, O, Fe, Ti, Al, Ca, and Mg, with direct remote sensing technique that can be widely used in lunar science. Optical techniques are also used to estimate chemical composition of the lunar regolith. Iron and titanium, being the main chromophore (transition) elements in the lunar material, are very important discriminators to classify lunar rocks and, therefore, their remote measurements draw attention of many workers. Recently a prospective and widely used approach to determine TiO_2 and FeO abundance in the lunar surface was suggested in [3,4,5]. Independent techniques for estimation of chromophore elements abundance were proposed in [6,7]. Owing to correlations between concentrations of the chromophores and other elements, e. g., Al, Ca, and Mg [8], there is an opportunity to map the elements using the Clementine UVVIS spectral reflectance (CSR) data [9], taking advantage of their high spatial resolution, up to 100 m for CSR. The CSR and GRS measurements provide information, respectively, from the upper 1 mm of the lunar surface and the upper 20 – 30 cm layer. Therefore integrating analyses of CSR and Lunar Prospector GRS data can provide more information about character and distribution of chemical elements on the lunar surface [10,11]. Unfortunately spatial resolutions of available CSR and GRS data are very different and, therefore, their comparison, which is very important, is not a simple task. We have suggested an empirical technique to interpolate available GRS data using CSR images acquired with UVVIS camera [12]. We consider the low resolution GRS data as a "Ground truth" to establish relationships linking optical mineralogy and geochemical information on the basis of the maximum of correlation. This permits the derivation of intermediate spatial resolution elemental abundance maps (Fe, Ti, O, Al, Ca, and Mg maps) by means of available CSR mosaics.

GRS OPTICAL INTERPOLATION TECHNIQUE

Two lunar missions, Lunar Prospector (1999) and Clementine (1994), made it possible a global coverage of the lunar surface with optical and geochemical data. The CSR multispectral data available for five spectral bands: 750, 900, 950, 1000 nm. These bands overlap well-known 1-μm pyroxene feature in lunar spectra; this feature is mainly controlled by

Fe^{2+} abundance in the crystal lattices of major lunar minerals. As a first step we bring 5-bands CSR data to the GRS grid (approximately 5°x5°) using simple rebinning. Then using a set of optical characteristics (e.g., albedo, colour indexes, etc.), we formally correlate GRS data with a combination of the optical characteristics and find regression parameters providing the maximal correlation coefficients.

Many various linear / non-linear combinations of optical parameters can be chosen to find a rule for interpolation of GRS data. Well-known empirical combinations using albedos at three wavelengths 415, 750 and 950 nm for prediction of Fe and Ti abundance were presented by Lucey et al. [3,4]. This method is developed only for two chromophore chemical elements prediction and does not use all available wavelengths in CSR data set. We developed Lucey's formulation considering a formal non-linear combination of different albedo as the following:

$$P = q\left\{\arctan\left[\frac{A(\lambda_1)/A(\lambda_2)-y}{A(\lambda_2)-x}\right]\right\}^s + p\,, \qquad (1)$$

where P is a geochemical parameter (we use below Fe or Ti abundance in weight %), $A(\lambda)$ is the albedo (%) at a given wavelength λ. For estimates of iron content we use albedo at λ_1 = 950 nm and λ_2 = 750 nm. For titanium the wavelengths are λ_1 = 415 nm and λ_2 = 750 nm. Correlation analysis gives a set of optimal coefficients q, p, s, x, and y providing maximal correlation of predicted and GRS data. Another empirical combination of spectral parameters has been applied in [13,14] to map chemical and mineral composition, using the CSR data (UVVIS 5 bands) at 1 km resolution, and data of the Lunar Soils Characterisation Consortium [15] for mare lunar soils. This combination is:

$$\log P = aA_R + bC_{BR} + cC_{IR1} + hC_{IR2} + fC_{IR3} + eD + g, \qquad (2)$$

where P is a geochemical parameter (Fe, Ti, O, Al, Ca, or Mg abundance in weight %), $A_R = A$(750 nm), in %; $C_{BR} = A$(415 nm) / A(750 nm), $C_{IR1} = A$(900 nm) / A(750 nm), $C_{IR2} = A$(950 nm) / A(750 nm), $C_{IR3} = A$(1000 nm) / A(750 nm), $D = A$(750 nm) A(1000 nm) / $[A(900\text{ nm})]^2$, and the coefficients *a, b, c, h, f, e,* and g should provide the maximal correlation coefficients in correlations with the GRS "Ground truth" data. Relationship (1,2) between the GRS and optical data is used to derive elemental abundance maps for Fe and Ti, O, Al, Ca, and Mg distributions with an improved spatial resolution. We use maps of Fe, Ti, O, Al, Ca, Mg acquired during the high-altitude portions of the Lunar Prospector mission (the versions of June 15, 2002, http://pds-geosciences.wustl.edu/missions/lunarp/reduced.html). The map bin size is approximately 5° by 5° (i.e. 150 km by 150 km). We treat these maps as a "Ground truth" to obtain coefficients q, p, s, x, y and *a, b, c, h, f, e, g.* Using the least-square method we search for the maximal correlation coefficients k for relationships between the "Ground truth" data and the parameter P minimising the deviation of prediction from GRS data. The values of the coefficients are given in Table 1 for Eq. (1) and Table 2 for Eq. (2), respectively. The correlation coefficients corresponding to the linear central regression are fairly high (see Tables 1,2), especially for iron. As can be seen the correlation coefficients for Fe is higher if apply an Eq. 2 for prediction; that is why we use below only Eq. (2) for Fe prognosis; the same is observed for O, Al, Ca, and Mg. In contrast, Equation 1 provides the linearity and higher correlation coefficient for Ti. The worst correlation is observed for Ca. We have estimated uncertainties of such a determination of chemical abundance. For example, the Ti uncertainties are +1.4, -0.6 wt% at the average 2 wt % that is rather typical for the Ti determinations with optical techniques (e.g., [5, 16]).

MAPS FOR CHEMICAL ELEMENTS

Iron. Figure 1 presents maps regarding the iron distribution. The upper image is the initial GRS data. The lower one is a prediction for iron distribution obtained with Equation (1) for the spatial resolution 15 km. The color map in Figure 1 and maps hereafter were made using superposition of the parameter distribution (color-coded) with the CSR 750 nm grey-scaled albedo distribution. Our Fe map with 15 km pixel looks very similar to the published maps with analogous content (e.g., [4, 5, 11]). Detailed comparison of distributions of optically determined ([4,5]) and new interpolated GRS iron with 15-km pixels gives a basis for additional information concerning composition of several lunar regions. Maria of the lunar nearside have lower abundance of iron determined with the optical algorithm. The same is observed for the north highland of the farside. In contrast, South Pole – Aitken Basin and regions supposed to be cryptomaria (Schickard – Schiller region), and highlands surrounding the nearside maria are characterised with relatively high values of iron concentration estimated with the optical method. The discrepancies found for the South Pole – Aitken Basin are in agreement with earlier studies [10,11] supporting the suggestion about impact excavation of deep crustal and mantle materials in the formation of the Basin [17]. Highlands on the new map have typical values of Fe content

near 4 %. Mare regions, such as Procellarum Ocean, Mare Tranquillitatis, Mare Serenitatis, and Mare Imbrium, show significantly higher content of Fe than highlands; the same is observed for the South Pole – Aitken Basin. The Fe map reveals abnormalities related to large young craters containing immature soils. Owing to that the mare regions are inhomogeneous.

Titanium. Figure 2 show results for mapping of titanium. The nearside portion of the color map presented in Fig. 2 looks qualitatively close to published ones [5,6,18]. In particular the well-known titanium difference between Mare Serenitatis and Mare Tranquillitatis is clearly seen for all the mentioned maps. The highland regions are fairly homogeneous with typical values of titanium content near 0.3 %. Comparison of previously determined titanium [4,5] and interpolated GRS reveal that the scale of GRS titanium is stretched in comparison with the previous estimates. That is, on average, at high concentrations of Fe and Ti the optical prognosis underestimates iron and overestimates titanium concentrations in comparison with the GRS technique. We study also correlation between the new iron and titanium distributions. This study reveals a close non-linear correlation between these elements, which is in agreement with our previous results [6,8]. The Ti-Fe correlation diagram for our prognosis and the initial Lunar Prospector data demonstrate good coincidence.

Note another difference of our chromophore (Fe,Ti) elements mapping results from Lucey's optical technique [3,4]. Lucey's method has a limitation in the domain of high values of iron content, whereas the interpolated GRS data allow the values higher than 20% that is in agreement with conclusions in [10]. Analogous results we obtained for titanium: there is a non-linear correlation between the pure optical and interpolated GRS predictions. The interpolated GRS data show less values of Ti content in the high titanium domain as compared to Lucey's optical determinations. The same difference was obtained in [19].

Non-chromophore elements. Figures 3–6 present maps for O, Al, Ca, Mg, respectively. The lower panels present results of our interpolations. One can expect false details in areas with young craters as they contain immature soils because of the Clementine UVVIS data are strongly influenced with variations of the maturity degree of the lunar soils. However, the obtained maps are fairly smooth and do not reveal big abnormalities related to young craters. An exception is the Mg distribution. We emphasize once more that though the listed elements are not chomophores, they correlate with optical parameters through iron and titanium. In addition, spectral properties of the lunar regolith are formed with minerals, not with elements. An important factor influencing the intensity and position of absorption bands is the distances between ions in the crystalline lattice of minerals. Non-transition elements change the lattice distances affecting in that way the optical spectra. For example, Ca in pyroxenes noticeably changes the positions of the crystal-field bands near 1 μm and 2μm, though it is not transition element. Thus we believe that these points support the reliability of maps of such elements as Ca, Mg, and others.

The oxygen distribution is generally correlated with abundance of iron and titanium, as ultrabasic rocks contain usually more Fe and Ti than basic ones. We note several prominent anomalies of the oxygen distribution. They are associated with the South Pole – Aitken Basin, the Schickard – Schiller region, and the crater Tycho. We note also a subtle regional structure in Procellarum Ocean that corresponds to lava flows of different ages. The distribution of aluminum abundance (see Figure 4) resembles an albedo image with noticeable suppressing of bright craters and their ray systems. Thus the aluminum distribution strongly anti-correlates with the iron content. This result is consistent with numerous laboratory studies of lunar samples (e.g., [15,20]). The distribution of calcium (see Figure 5) shows low contrast mare/highland, though all maria are clearly seen. Higher content of Ca is observed for the equatorial regions of the farside. Figure 6 presents magnesium abundance. Mare regions are inhomogeneous for this parameter. Some bright mare craters can be seen in the map. That is perhaps a demonstration of shortcomings of our technique that cannot be always applicable for areas with immature regolith. Concentrations of calcium and magnesium are globally anti-correlated. More detailed consideration of the correlation Mg-Ca reveals two strongly overlapped branches.

CONCLUSION

Our scheme representing the current status of thematic cartography of the Moon (e.g. Fig.1 in [21]) implies several types of lunar thematic maps. In this work we have presented new maps of chemical elements abundances over lunar surface.

1. We suggest an empirical approach for optical interpolation of available GRS data. Our technique allows one to derive elemental abundance maps from Lunar Prospector data for such elements as Fe, Ti, O, Al, Ca, and Mg at an improved resolution, intermediate between those of GRS and CSR data (with a potential gain of a factor of 10) permitting regional geologic investigations. The main limitation of the technique is its dependence on how well the abundance of the elements correlates with the Clementine UVVIS data.

2. The new iron and titanium maps exhibit non-linear relationships with corresponding distributions obtained with Lucey's technique. These maps are consistent with previous works (e.g., [10,11]). We confirmed reliability of our approach with the correlation between the predicted iron distribution and measured one using in both these cases the maps with 15-km pixels. The maps of non-chromophore elements, O, Al, Ca, and Mg appear to be very informative. For example, the map of oxygen demonstrates an anomaly in the crater Tycho, and the map of calcium shows very low mare/highland contrast.

3. We plan to investigate of correlations between the chemical elements and classify the lunar surface with these correlations (cluster analyses). Also we plan to present a detailed geological description of the new maps. The technique described above can be easily applied to AMIE/D-CIXS/Smart-1 [22,23] data in order to increase spatial resolution of lunar compositional maps.

REFERENCES.

[1] Feldman, W. C., et al., 1999. The Lunar Prospector gamma-ray and neutron spectrometers. Nuclear Instruments and Methods in Physics Research A, 422, 562.

[2] Prettyman, T. H., et al., 2002. Library least squares analysis of Lunar Prospector gamma-ray spectra. Lunar and Planetary Science Conf. 33rd. Abstract #2012. LPI Houston.

[3] Lucey, P., et al., 1998. Mapping the FeO and TiO_2 content of the lunar surface with multispectral imagery. J. Geophys. Res. 103, 3679-3700.

[4] Lucey, P. G., et al., 2000 a. Lunar iron and titanium abundance algorithms based on final processing of Clementine ultraviolet-visible images. J. Geophys. Res. 105, 20,297-20,306.

[5] Blewett, D. T., et al., 1997. Clementine images of the lunar sample-return stations: Refinement of FeO and TiO_2 mapping techniques. J. Geophys. Res. 102, 16319-16326.

[6] Shkuratov, Yu. G., et al., 1999. Iron and titanium abundance and maturity degree distribution on lunar nearside. Icarus, 137, 222-234.

[7] Le Mouélic, S., et al., 2000. Discrimination between maturity and composition of lunar soils from integrated Clementine UVVIS-NIR data. Application to Aristarchus Plateau. J. Geophys. Res., 105 (E4), 9445-9455.

[8] Pieters, C. M., et al., 2002. Statistical analysis of the links between lunar mare soil mineralogy, chemistry and reflectance spectra. Icarus, 155, 285-298.

[9] Eliason, E. M., et al., R., 1999. To the Moon: the Clementine UVVIS global mosaic. US Geol. Surv., Flagstaff, Ariz.

[10] Lawrence, D. J., et al., 2002. Iron abundances on the lunar surface as measured by the Lunar Prospector Gamma-Ray and Neutron Spectrometers. J. Geophys. Res., 107, E12, 10.1029/2001JE001530.

[11] Chevrel, S., et al., 2002. Integration of the Clementine UV-VIS spectral reflectance data and the Lunar Prospector gamma-ray spectrometer data: A global-scale multi-element analysis of the lunar surface using iron, titanium, and thorium abundance. J. Geophys. Res. 107, No. E12, 10.1029/2000JE001419.

[12] Shkuratov, Yu., et al., 2004. Derivation of elemental abundance maps at 15-km spatial resolution from the merging of Clementine optical and Lunar Prospector geochemical data. Lunar Planet. Sci. 35th. Abstract # 1162. LPI Houston.

[13] Shkuratov, Yu., et al., 2003. Estimates of the lunar surface composition with Clementine images and LSCC data. Lunar Planet. Sci. Conf. 34th. Abstract # 1258. LPI Houston.

[14] Shkuratov, Yu., et al., 2003. Composition of the lunar surface as will be seen from SMART-1: A simulation using Clementine data. J. Geophys. Res., 108, (E4), 10.1029/2002JE001971.

[15] Taylor, L. A., et al., 2001. Lunar mare soils: Space weathering and the major effects of surface-correlated nanophase Fe. J. Geophys. Res., 106, 27,985-28,000.

[16] Gillis, J., et al., 2003. A revised algorithm for calculating TiO_2 from Clementine UVVIS data: A synthesis of rock, soil, and remotely sensed TiO_2 concentrations. J. Geophys. Res., 108, E2, 10.1029/2001JEoo1515.

[17] Head, J., et al., 1993. Lunar impact basin: New data for the western limb and farside (Orientale and South Pole – Aitken basin) from the first Galileo flyby. J. Geophys. Res. 98, 17,149-17,181.

[18] Johnson, J. R, et al., 1991. Remote sensing of potential lunar resource: 1. Near-side compositional properties. J. Geophys. Res. 96, 18861-18821.

[19] Elphic, R. C., et al., 2002. Lunar Prospector neutrons spectrometer constraints on TiO_2. J. Geophys. Res., 107 (#E4), 10.1029/2000JE001460.

[20] Pieters, C., Taylor, L., 2003. Systematic global mixing and melting in lunar soil evolution. Geophys. Res. Lett. 30. No 20, 2048. doi: 10.1029/2003 GL 018212.

[21] V. Kaydash and Yu. Shkuratov, 2004. Frontiers of the thematic cartography of the Moon // Proc. of int. sci.-techn. Conf. devoted to 255 anniversary of MIIGAiK, pp. 396-400. Moscow.

[22] Dunkin, S.K., et al., 2003. Scientific rationale for the D-CIXS X-ray spectrometer on board ESA's SMART-1 mission to the Moon. Planet. and Space Sci. 51, 435 – 442.

[23] Josset, J.-L., et al., 2002. Asteroid Moon micro-Imager Experiment (AMIE) for SMART-1 Mission, Science Objectives and Development Status. EGS XXVII General Assembly, Nice, France, April 2002, abstract #EGS02-A-06862.

Table 1. Coefficients of equation (1) found with the GRS-interpolating technique (*k* is the correlation coefficient).

	q	*p*	*x*	*y*	*s*	*k*
Ti	2.77	-0.69	0	0.42	3	0.90
Fe	-11.23	-2.41	0.08	1.16	1	0.92

Table 2. Coefficients of equation (2) found with CSR and GRS data (*k* is the correlation coefficient).

	a	*b*	*c*	*h*	*e*	*f*	*g*	*k*
Ti	-0.090	8.303	-95.841	0.72	43.169	-44.783	93.31	0.86
Fe	-0.039	1.354	-38.321	0.314	16.251	-18.2	40.819	0.96
Al	0.020	-1.029	34.5	-0.174	-15.217	17.34	-35.26	0.76
Ca	0.020	-1.581	32.747	-1.425	-14.613	14.369	-29.523	0.67
Mg	-0.031	1.217	-25.209	2.161	10.101	-5.940	19.47	0.73
O	0.0015	-0.069	7.910	0.148	-3.676	4.217	-6.966	0.75

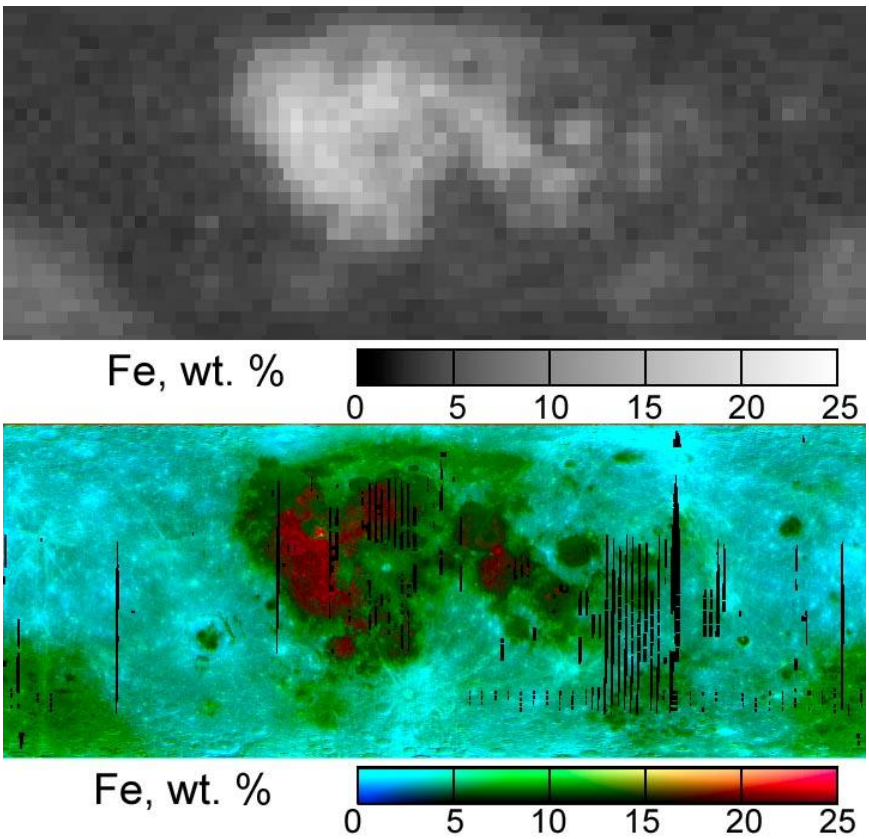

Figure 1. Iron distribution over the lunar surface. Upper map and lower map correspond to the initial GRS data and the result of applying equation (2). The map projection is simple-cylindrical.

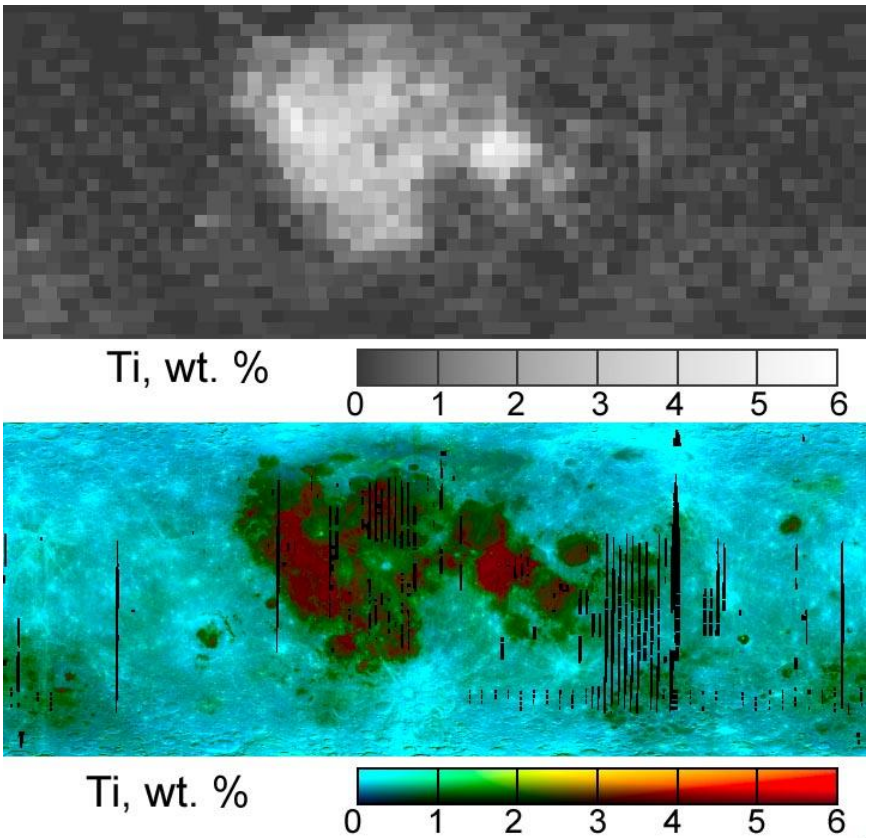

Figure 2. Titanium distribution over the lunar surface. Upper map and lower map correspond to the initial GRS data and the result of applying equation (1). The map projection is simple-cylindrical.

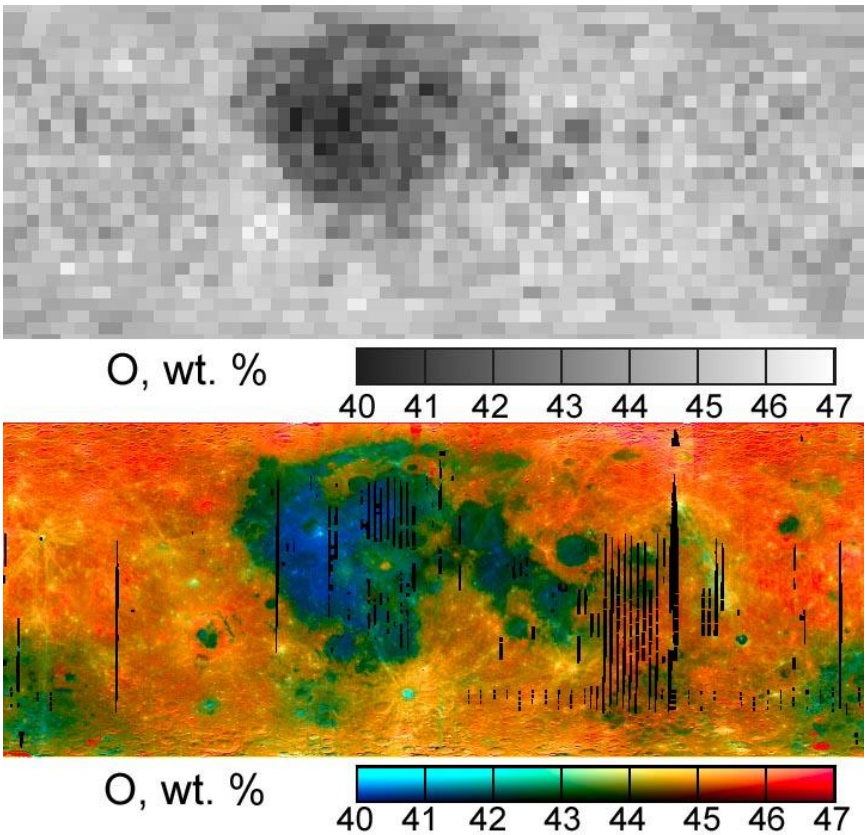

Figure 3. Oxygen distribution over the lunar surface. Upper map and lower map correspond to the initial GRS data and the result of applying equation (2). The map projection is simple-cylindrical.

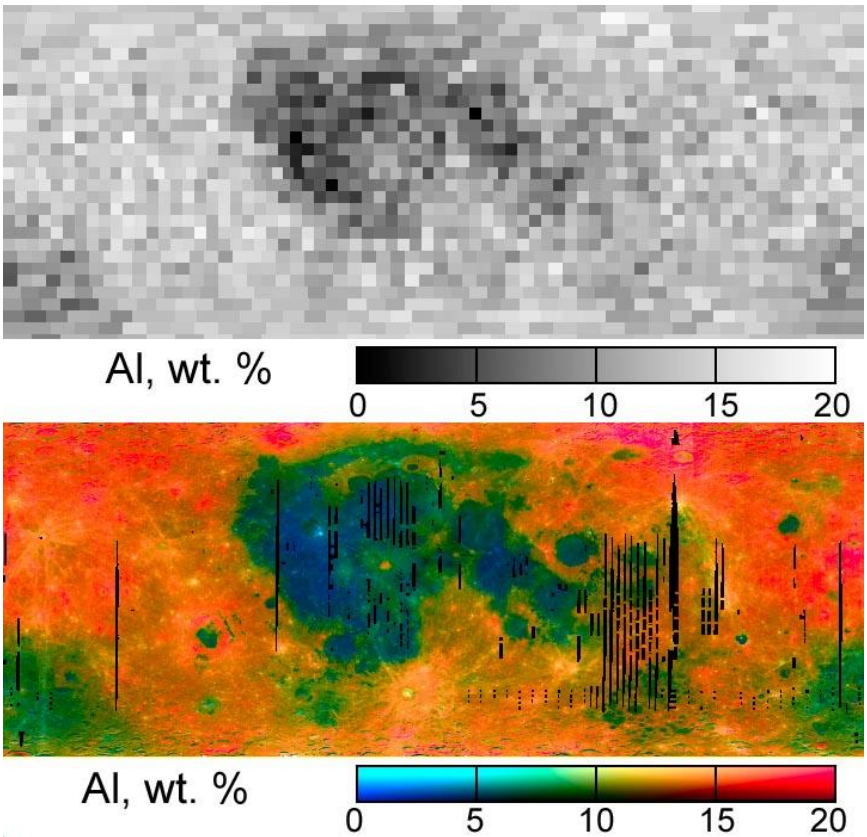

Figure 4. Aluminium distribution over the lunar surface. Upper map and lower map correspond to the initial GRS data and the result of applying equation (2). The map projection is simple-cylindrical.

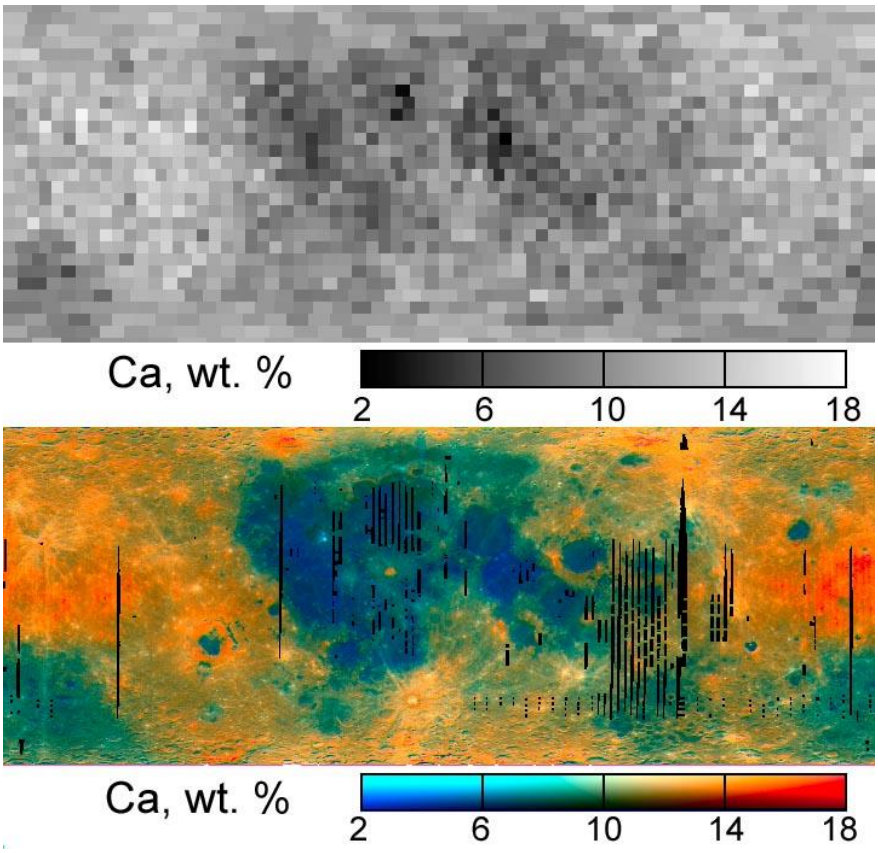

Figure 5. Calcium distribution over the lunar surface. Upper map and lower map correspond to the initial GRS data and the result of applying equation (2). The map projection is simple-cylindrical.

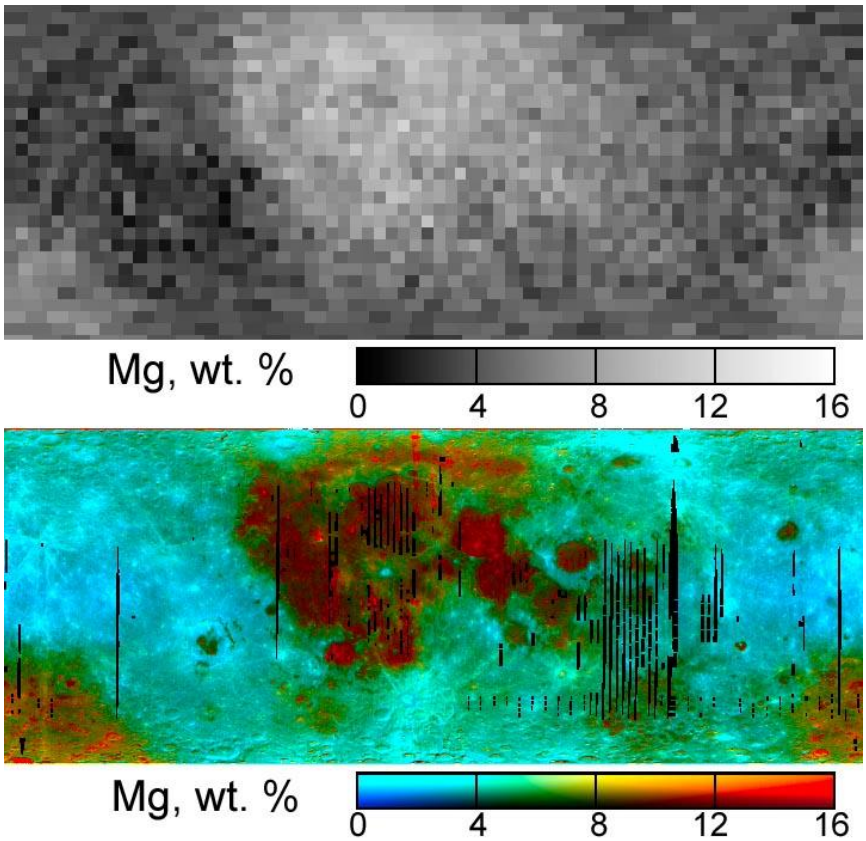

Figure 6. Magnesium distribution over the lunar surface. Upper map and lower map correspond to the initial GRS data and the result of applying equation (2). The map projection is simple-cylindrical.

BIOGRAPHY OF THE PRESENTING AUTHOR

Vadym G. Kaydash

Dr. Vadym G. Kaydash
Astronomical Institute of
Kharkov National University,
Sumskaya St., 35,
Kharkov, 61022
Ukraine
e-mail: kvg@vk.kh.ua
Tel:+38-057-707-50-63
FAX:+ 38-057-700-53-49

Personal data

Date and place of birth: October 9, 1971, Kharkov, Ukraine **Sex:** male
Nationality: Ukraine

Education:

- 1998 Ph.D. from Main Astronomical Observatory, Natl. Acad. Sci. of Ukraine, Kiev, Ukraine. Thesis "Prediction of the Chemical Content and Zoning of the Lunar Nearside Surface by Optical Measurements Data"
- 1993 M.S. in physics and astronomy and in M.S. in physics and astronomy teaching Department of Physics, Kharkov National University.

Positions:

- 2005 assistant professor, Physics Department, Kharkov National University
- Since 1999 Research scientist, Department of Remote Sensing of Planets, Astronomical Institute, Kharkov National University
- 1997 - 1998 Engineer, Department of Remote Sensing of Planets, Astronomical Institute, Kharkov National University
- 1993 - 1997 Astronomy teacher, Kharkov city children's palace of culture, Ukraine

Expertise:

- Planetary astrophysics
- Image processing

Recent research activities are related to analysis and interpretation of astronomical and spaceborne data on planetary surfaces.

Selected papers:

Y. Shkuratov, G. Videen, M. Kreslavsky, I. Belskaya, V. Kaydash, A. Ovcharenko, V. Omelchenko, N. Opanasenko, E. Zubko. Scattering properties of planetary regoliths near opposition. In: *Photopolarimetry in Remote Sensing* / Eds. G. Videen, Ya. Yatskiv, and M. Mishchenko. NATO Science Series. Kluwer Academic Publishers, London. Series II, Vol. 161, pp. 191-208 (2004).

The SMART-1 Mission: Photometric Studies of the Moon with the AMIE Camera Yu. G. Shkuratov, M. A. Kreslavsky, D. G. Stankevich, V. G. Kaydash, P. Pinet, V. V. Shevchenko, B. H. Foing, and J.-L. Josset //Solar System Research, p. 251-259, v. 37, N. 4 (2003)

Shkuratov Yu.G., Stankevich D.G., Kaydash V.G.,Omelchenko V.V., Pieters C.M., Pinet P.C., Chevrel S.D.,Daydou Y.H., Foing B.H., Sodnik Z., Josset J.-L., Taylor L.A., Shevchenko V.V. Composition of the lunar surface as will be seen from SMART-1: A simulation using Clementine data, J. Geophys. Res. Planets. Vol. 108 No. E4. 10.1029/2002JE00197103 (2003)

V. Kaydash, Yu. Shkuratov, M. Kreslavsky, K. Muinonen, J. Piironen, P. Pinet, Chevrel S., Daydou Y., Shevchenko V.V., B. Foing, J.-L. Josset. Processing and analysis of phase ratio images from SMART-1 and Clementine. In Heather D.J. (ed) New Views of The Moon, Europe: Future Lunar Exploration, Science Objectives and Integration of Datasets. ESTEC RSSD, Noordwijk. (2002)

Kreslavsky, M.A., Shkuratov, Yu.G., Velikodsky, Yu.I., Kaydash, V.G., Stankevich, D.G., Pieters, C.M. Photometric properties of the lunar surface derived from Clementine observations // J. Geophys. Res. Planets. Vol. 105 , No. E8 , p. 20,281. (2000)

Shkuratov Yu.G., Kaydash V.G., Opanasenko N.V. Iron and titanium abundance and maturity degree distribution on lunar nearside. Icarus, 137, No. 2, 222-234. (1999)